NEURAL REGENERATION RESEARCH
June 2015, Volume 10, Issue 6
www.nrronline.org

RESEARCH ARTICLE

In vivo tracking of human adipose-derived stem cells labeled with ferumoxytol in rats with middle cerebral artery occlusion by magnetic resonance imaging

Yan Yin[1], Xiang Zhou[2], Xin Guan[3], Yang Liu[4], Chang-bin Jiang[2, *], Jing Liu[4, *]

1 Department of Neurology, the Second Affiliated Hospital of Dalian Medical University, Dalian, Liaoning Province, China
2 Department of Neurology, the First Affiliated Hospital of Dalian Medical University, Dalian, Liaoning Province, China
3 College of Life Sciences, Liaoning Normal University, Dalian, Liaoning Province, China
4 Regenerative Medicine Center, First Affiliated Hospital of Dalian Medical University, Dalian, Liaoning Province, China

***Correspondence to:**
Chang-bin Jiang or Jing Liu, M.D., jchangbinvip@163.com or liujingdalian@163.com.

***doi:**10.4103/1673-5374.158355*
***http:**//www.nrronline.org/*

***Accepted:** 2015-03-11*

Abstract

Ferumoxytol, an iron replacement product, is a new type of superparamagnetic iron oxide approved by the US Food and Drug Administration. Herein, we assessed the feasibility of tracking transplanted human adipose-derived stem cells labeled with ferumoxytol in middle cerebral artery occlusion-injured rats by 3.0 T MRI *in vivo*. 1×10^4 human adipose-derived stem cells labeled with ferumoxytol-heparin-protamine were transplanted into the brains of rats with middle cerebral artery occlusion. Neurologic impairment was scored at 1, 7, 14, and 28 days after transplantation. T2-weighted imaging and enhanced susceptibility-weighted angiography were used to observe transplanted cells. Results of imaging tests were compared with results of Prussian blue staining. The modified neurologic impairment scores were significantly lower in rats transplanted with cells at all time points except 1 day post-transplantation compared with rats without transplantation. Regions with hypointense signals on T2-weighted and enhanced susceptibility-weighted angiography images corresponded with areas stained by Prussian blue, suggesting the presence of superparamagnetic iron oxide particles within the engrafted cells. Enhanced susceptibility-weighted angiography image exhibited better sensitivity and contrast in tracing ferumoxytol-heparin-protamine-labeled human adipose-derived stem cells compared with T2-weighted imaging in routine MRI.

***Key Words:** nerve regeneration; brain injury; neuroimaging; ferumoxytol; superparamagnetic iron oxide particles; human adipose-derived stem cells; middle cerebral artery occlusion; intracerebral injection; magnetic resonance imaging; enhanced susceptibility-weighted angiography image; modified neurological severity scores; rats; Prussian blue staining; neural regeneration*

***Funding:** This study was supported by the Science and Technology Plan Project of Dalian City in China, No. 2014E14SF186.*

Yin Y, Zhou X, Guan X, Liu Y, Jiang CB, Liu J (2015) In vivo tracking of human adipose-derived stem cells labeled with ferumoxytol in rats with middle cerebral artery occlusion by magnetic resonance imaging. Neural Regen Res 10(6):909-915.

Introduction

Stroke is a leading cause of mortality and long-term disability, with no effective treatments because of a limited regenerative capacity of the damaged central nervous system (Huang et al., 2012; Cromer Berman et al., 2013). Stem cells, with the capacity to self-renew and differentiate into different cell types, provide hope for future cell-based regenerative therapies (Delcroix et al., 2009; Struys et al., 2013).

Multiple stem cells, such as bone marrow mesenchymal stem cells (Arslan et al., 2013; Huang et al., 2013), neural stem cells (Qu et al., 2013), and embryonic stem cells (Ma, 2013), have been tested as potential sources for cell-based therapy for ischemic stroke (Nagai et al., 2010; Seyed Jafari et al., 2011; Tae-Hoon and Yoon-Seok, 2012; Mine et al., 2013). Several lines of evidence indicate that adipose tissue may represent an ideal source for stem cells: (1) the collection of adult adipose tissue is technically easy and safe (Liu et al., 2014); (2) the frequency of adipose-derived stem cells (ADSCs) in digested adipose tissue is approximately 500-fold higher that in freshly isolated bone marrow mesenchymal stem cells (Marconi et al., 2012); and (3) the possibility of transplantation with no immune rejections, ethical problems, or tumorigenesis (Kim et al., 2012). Moreover, ADSCs from mice, rats, nonhuman primates, and humans were demonstrated to differentiate into neural and glial cells *in vivo* and *in vitro* (Wei et al., 2009; Zhang et al., 2014).

MRI is a non-invasive tool that has a high sensitivity for cell tracking, with superparamagnetic iron oxide (SPIO) particles the preferred material for magnetic labeling of cells (Song et al., 2009; Li et al., 2010). Ferumoxytol, a colloidal suspension of carbohydrate-coated ultra-small superparamagnetic iron oxide nanoparticles (USPIO) (intravenous

iron formulation), is currently approved to treat iron deficiency anemia in patients with chronic kidney disease (Schiller et al., 2014). In the present study, we hypothesized that ferumoxytol cell labeling would allow tracking of hADSCs introduced into the brain of an experimental ischemic rat model using a clinical 3.0 T MRI. The objectives of our current study were to determine the optimal labeling combination among ferumoxytol-protamine, ferumoxytol-heparin-protamine (HPF), and ferumoxytol-poly-L-lysine nanocomplexes *in vitro*, to assess the effect of hADSCs for treatment of ischemic stroke, and to demonstrate the feasibility of tracking transplanted HPF-labeled hADSCs in middle cerebral artery occlusion (MCAO)-injured rats by MRI *in vivo* with the aim of advancing this technology to the clinic.

Materials and Methods

Animals

A total of 52 adult, clean, healthy, male, Sprague-Dawley rats, aged 10–12 weeks, weighing 250–300 g, were purchased from SPF Animal Center, Dalian Medical University (license No. SCXK(Liao) 2013-0003), China. Prior to experimentation, rats were given a normal diet for 7 days to acclimatize to vivarium conditions, in a room controlled at 23 ± 1°C and maintained in an alternating 12-hour light/dark cycle. All experimental procedures were conducted in accordance with the *Guidance Suggestions for the Care and Use of Laboratory Animals*, issued by the Ministry of Science and Technology of China.

Adipose tissue

Human adipose tissue samples isolated *via* lipoaspiration from healthy female donors (age range: 32–42 years) were obtained from the Second Hospital of Dalian Medical University in China with the approval of patients. All studies were approved by the ethics committee of Dalian Medical University in China.

Animal groups

Twelve rats died or were unsuccessful models, and 40 successful models were randomly divided into four groups (n = 10 for each group): control group (MCAO alone), PBS group, unlabeled-hADSCs group, and HPF-hADSCs group. In the control group, no other treatments were made after MCAO. The other three groups were treated with PBS, unlabeled-hADSCs, and HPF-hADSCs after MCAO, respectively.

Isolation and culture of hADSCs

hADSCs were isolated according to the method reported previously (Locke et al., 2009). Briefly, to remove debris and blood cells, excised adipose tissue was extensively washed three times with sterile PBS containing 1% penicillin and streptomycin. Subsequently, the adipose tissue was minced and digested with 1% collagenase I (Gibco, Carlsbad, CA, USA) at 37°C for 30–60 minutes. Collagenase activity was neutralized by adding 10% fetal bovine serum (Gibco). Cells were separated through a 200-mesh filter and centrifuged at 1,000 r/min for 5 minutes. After washing with sterile PBS, the hADSC pellet was resuspended in the complete medium (basal medium + 10% fetal bovine serum + 1% glutamine + 1% penicillin/streptomycin) and maintained at 37°C, 5% CO_2. The culture medium was changed every 3–4 days. The 80–90% confluent hADSCs were used for experiments (Zuk et al., 2001). hADSCs were recognized as described previously (Haddad-Mashadrizeh et al., 2013).

Cell labeling

Ferumoxytol (Feraheme, AMAG Pharmaceuticals, Waltham, MA, USA), heparin sulfate (Qianhong Biopharma, Changzhou, Jiangsu Province, China), protamine sulfate (Sigma, St. Louis, MO, USA), and poly-L-lysine hydrobromide (Sigma) were purchased commercially. Ferumoxytol, heparin sulfate, and poly-L-lysine hydrobromide were used to form nanocomplexes. Ferumoxytol-protamine nanocomplexes, HPF nanocomplexes, and ferumoxytol-poly-L-lysine nanocomplexes were prepared as previously described (Rice et al., 2007; Castaneda et al., 2011; Thu et al., 2012).

Ferumoxytol-protamine and HPF nanocomplexes were added to appropriate serum-free medium and incubated for 4 hours, whereas ferumoxytol-poly-L-lysine nanocomplexes were added to complete medium and incubated for 24 hours. After 4 hours, an equal amount of complete medium containing 20% fetal bovine serum was added to the ferumoxytol-protamine group and HPF group, and hADSCs were incubated for 10 and 20 hours, respectively. After incubation, labeled cells were washed sufficiently to remove excess complexes and examined *in situ* for labeling efficiency and viability. We used Prussian Blue staining to assess labeling efficiency (Arbab et al., 2009). hADSCs were fixed with 4% paraformaldehyde (Kaitong, Chemical Co., Tianjin, China) for 40 minutes, then washed three times with PBS and incubated with Perls' reagent (Kaitong, Chemical Co., Tianjin, China) at 37°C for 30 minutes. The cells were washed and observed under the microscope (Olympus, IX70, Tokyo, Japan). The labeling efficiency was calculated as the number of Prussian Blue-labeled cells over the total number of cells in the field.

Establishment of MCAO models and stem cell transplantation

The rats were anesthetized with 100 mg/kg chloral hydrate by intraperitoneal injection. Body temperature was maintained at 37°C after surgery by placing the animals under heat lamps. A No. 4-0 monofilament nylon suture with a silicone-coated tip was inserted through an arteriotomy in the right common carotid artery and gently advanced into the internal carotid artery to a point approximately 18 mm distal to the bifurcation of the carotid artery (Longa et al., 1989). After 90 minutes of transient occlusion, the cerebral blood flow was restored by withdrawal of the nylon thread. The rats were allowed to recover from the anesthesia and then placed back into the cages (one rat per cage) with free access to food and water. The rat was considered as a successful model when right Horner's sign and left-sided hemiparesis in the upper extremities with counterclockwise circling and

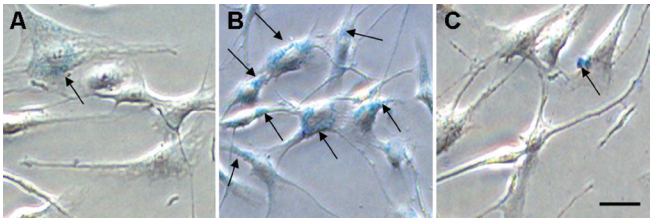

Figure 1 Labeling effects of PF, HPF, and F-PLL nanocomplexes in Prussian blue staining (light microscope).
Prussian blue staining of third passage hADSCs labeled with SPIO nanocomplexes (arrows indicate iron particles in cells). (A) hADSCs labeled with PF nanocomplexes (dimness in blue). (B) hADSCs labeled with HPF nanocomplexes (rich in blue). (C) hADSCs labeled with F-PLL nanocomplexes (blurry in blue). Scale bar: 25 μm. PF: Ferumoxytol-protamine; HPF: heparin-protamine; F-PLL: ferumoxytol-poly-L-lysine; hADSCs: human adipose-derived stem cells; SPIO: superparamagnetic iron oxide.

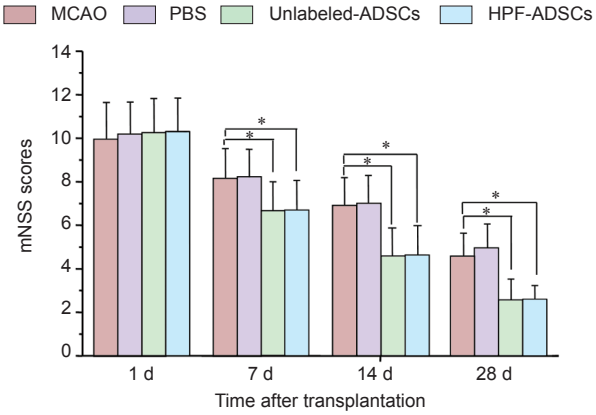

Figure 2 Neurological function changes in MCAO rats transplanted with ferumoxytol-labeled hADSCs (mNSS tests).
mNSS tests were performed at 1, 7, 14, and 28 days after transplantation. Data are expressed as the mean ± SD (n = 10). *P < 0.05. Statistical analyses were performed using one-way analysis of variance followed by the least significant difference test. MCAO: Middle cerebral artery occlusion; hADSCs: human adipose-derived stem cells; mNSS: modified neurological severity score; d: day(s).

rolling to the left side appeared, and T2-weighted imaging (T2WI) showed the lesion in the right hemisphere as a hyperintense area.

The animals were anesthetized as described above and mounted in a supine position on a stereotaxic apparatus. A hole with a diameter of 1 mm was drilled in the skull, and then PBS, unlabeled ADSCs, or ADSCs labeled with ferumoxytol (1×10^4 cells, 5 μL, for all) were injected into the right dorsolateral striatum 5 mm beneath the skull surface and 3 mm lateral to bregma over 5 minutes. The needle was left in position for 10 minutes. The hole was sealed with bone wax and the incision was disinfected and sutured. After transplantation, 8×10^6 U penicillin was injected into the rat muscle. All rats were returned to their separate cages and fed. The 40 rats were all alive after transplantation until 28 days.

Neurological function assessment

Animal behavior was assessed at 1, 7, 14, and 28 days after transplantation. All rats were evaluated using a modified neurological severity score (Chen et al., 2001), a composite of motor (muscle status, abnormal movement), sensory (visual, tactile, proprioceptive), reflex, and balance tests. Neurological function was graded on a scale of 0–18 (normal score, 0; maximal deficit score, 18). A higher score represents more severe injury.

MRI examination

MRI scanning was performed at 1, 7, 14, and 28 days after ADSCs transplantation. For all MRI scans, animals were placed in a supine position in a 3.0 T clinic unit (GE, Signa HDxt, Fairfield, CT, USA) with their heads fixed in a custom-made 8-channel surface coil designed for the rat brain. The imaging protocol consisted of fast spin echo T2WI and enhanced susceptibility-weighted angiography imaging. The sets of images were obtained with the following parameters: T2WI: field of view = 6.0 cm × 4.2 cm, repetition time = 3,240 ms, echo time = 89 ms, thickness = 3 mm, slice space = 0, flip angle = 90°, number of excitations = 6, matrix 256 × 192; enhanced susceptibility-weighted angiography imaging: field of view = 8.0 cm × 8.0 cm, repetition time = 50 ms, echo time = 3.2 ms, thickness = 2.3 mm, slice space = 0, flip angle = 15 °, number of excitations = 0.654, and matrix 256 × 192.

Histomorphometric evaluation

Rats were anesthetized and perfused at 28 days post-transplantation through the heart with cold saline and 4% paraformaldehyde, and brains were harvested for histological examination. A coronal section was made through the needle entry site and was then fixed in paraffin. Sections of 5 μm thickness were cut and stained with Prussian blue. For Prussian blue staining, slides were placed in a Coplin jar containing a 2:1 mixture of 2% potassium ferrocyanide and 2% hydrochloric acid (Kaitong, Chemical Co., Tianjin, China) for 30 minutes, rinsed with distilled water, counterstained with neutral red (Solarbio, Beijing, China) for 20 minutes, then examined by light microscopy (Leica, DM4000B, Ernst-Leitz-Strasse, Wetzlar, Germany).

Statistical analysis

Data are expressed as the mean ± SD. Statistical analyses were performed by one-way analysis of variance followed by the least significant difference test, using PASW Statistics 17 for Mac software (SPSS, Chicago, IL, USA). P < 0.05 was considered statistically significant.

Results

Labeling effects of SPIO on hADSCs

The superparamagnetic iron oxide (SPIO) nanocomplexes entered hADSCs by adsorption and endocytosis. The results of Prussian blue staining revealed that the particles of SPIO nanocomplexes mainly existed in the cytoplasm, stained blue in **Figure 1** (30 minutes after Prussian blue staining). Treatment with HPF nanocomplexes resulted in a maximum labeling rate of 99.32% ($n \geq 3$) (**Figure 1B**). By contrast, the labeling efficiency of ferumoxytol-protamine or ferumoxytol-poly-L-lysine nanocomplexes was very low (23.04%, 6.95%, respectively), and the staining was not obvious (**Figure 1A**, **C**).

Behavioral changes in MCAO rats transplanted with ferumoxytol-labeled hADSCs

Modified neurological severity score tests were conducted to assess the neurological functional recovery after stroke in rats. The difference score decreased in all four groups during the observation period ($P = 0.000$). No significant difference was found between the control (MCAO-alone) and PBS groups, or between the unlabeled-hADSCs and HPF-hADSCs groups, at any time point ($P = 0.865$). Similar to the unlabeled-hADSCs group, the HPF-hADSCs group exhibited a significant reduction in the post-treatment mean difference score compared with the control group at 7, 14, and 28 days ($P = 0.000$; **Figure 2**).

MRI tracking of hADSCs after transplantation in rats

MRI was used to serially monitor the MCAO-induced lesion in the right hemisphere, with T2WI images clearly showing the lesion in the right hemisphere as a hyperintense area at all time points (**Figure 3** upper).

MRI also allowed visualization of the behavior of transplanted hADSCs labeled with HPF nanocomplexes. A low signal change was obvious at the transplanted sites in T2WI at 1 day post-injection. After 28 days, the low signal intensity still presented at the transplanted sites, but became slightly blurred (**Figure 3** upper). The enhanced susceptibility-weighted angiography images showed a remarkably low signal change and a dark appearance in the right hemisphere (**Figure 3** lower), and remained stable even after 28 days. No signal changes were found in the contralateral hemisphere at any time point. In the unlabeled-hADSCs group, the low signal intensity by MRI was only observed on the first day, but was undetected thereafter. No hypointense signal changes were observed in the MCAO-alone or PBS groups in T2WI and enhanced susceptibility-weighted angiography images.

Prussian blue staining of tissue sections

The majority of the Prussian blue-stained cells had a round or oval shape, and were observed in brain tissue sections at or around the injection site in the HPF-hADSCs group (**Figure 4A**), which matched the hypointense areas on T2WI and enhanced susceptibility-weighted angiography images. Some blue iron particles were located in the ischemic cortex (**Figure 4B**) and a few diffuse particles observed in the ipsilateral subarachnoid space (**Figure 4C**). No Prussian blue-positive cells were present in the corpus callosum or the contralateral hemisphere in HPF-hADSCs, or in any region in the other three groups (**Figure 4D**).

Discussion

SPIO nanoparticles are a promising tool for labeling and tracking various cell types *in vivo* by MRI. Feridex (Endorem®-Europe; Guerbet, Sulzbach, Germany; Villepinte, France) or Feridex® in the USA and Japan (AMAG Pharmaceuticals, Waltham, MA, USA), a US Food and Drug Administration-approved SPIO nanoparticle contrast agent, was used in a number of stem cell tracking studies, an "off-label" use that nevertheless has been widely utilized (Edmundson et al., 2013). Unfortunately, ferumoxides and similar SPIO nanoparticles are no longer manufactured for commercial reasons, thus slowing the progress toward translating clinically approved agents for labeling and tracking cells by MRI into clinical trials. Recently, ferumoxytol, a semisynthetic carbohydrate non-dextran-coated USPIO, was approved for treatment of iron-deficiency anemia in chronic kidney disease. Since stem cells lack phagocytic capacity, transfection agents such as poly-L-lysine and protamine are typically used to internalize SPIO particles (Fu et al., 2011; Qi et al., 2013).

In the present study, we first labeled hADSCs with ferumoxytol combining protamine, heparin-protamine, and poly-L-lysine to determine the optimal labeling combination. We found that HPF nanocomplexes labeled hADSCs more efficiently compared with ferumoxytol-protamine and ferumoxytol-poly-L-lysine nanocomplexes. Moreover, HPF-labeled hADSCs could be clearly visualized by clinical 3.0 T MRI after intracerebral transplantation into rats. One of the main advantages of labeling stem cells with HPF nanocomplexes is that ferumoxytol, heparin, and protamine are used clinically. Thus, extensive safety testing of the drugs should not be necessary, and the time required for evaluating the use of HPF clinically should be shortened.

Although the majority of strokes are ischemic, reperfusion and anti-thrombotic therapies are of limited benefit (Del Zoppo et al., 2009; Liu, 2012). Recent advances in stem cell research show promise for stem cell-based treatments as a novel therapeutic strategy for ischemic stroke (Egashira et al., 2012). hADSCs can be isolated in large quantity and minimally invasively from the subcutaneous adipose tissue collected by liposuction (Fiedler et al., 2013), and the harvesting of hADSCs is free of ethical concerns. Thus, compared with other stem cells, hADSCs are more practical for use in clinical applications (Egashira et al., 2012). Moreover, ADSCs have the ability to differentiate into neuronal or vascular lineages both *in vivo* and *in vitro,* and these stem cells are expected to be useful in the replacement of injured neuronal cells and in restructuring of neuronal networks (Locatelli et al., 2009; Savitz et al., 2011). As such, hADSCs show potential as therapeutic agents in stroke management.

Experimentally, transplantation of bone marrow mesenchymal stem cells was reported to enhance functional recovery after MCAO in rats (Kawabori et al., 2012, 2013; Miyamoto et al., 2013). In the present study, stereotaxic transplantation of either unlabeled or HPF-labeled hADSCs into MCAO-injured rats resulted in improved neurological functional performance. A previous study on rodent ADSCs engraftment showed a similar improvement (Kang et al., 2003). The potential mechanisms of cell-based therapy-induced neurorestorative effects after stroke included cell replacement (De Feo et al., 2012; Oki et al., 2012; Emborg et al., 2013; Jensen et al., 2013), enhanced trophic/regenerative support from transplanted cells, immunomodulation, and stimulation of endogenous brain repair processes (such as angiogenesis, neurogenesis, synaptogenesis, neurovascular niche, and white matter remodeling) (Jin et al., 2011; Cho et al., 2012; Egashira et al., 2012; Franco et al., 2012; Kokaia

et al., 2012; Leong et al., 2012; Kocsis and Honmou, 2012; Smith and Gavins, 2012; van Velthoven et al., 2012; Wei et al., 2012; Inoue et al., 2013; McGuckin et al., 2013; Mine et al., 2013).

The successful translation of stem cell therapies requires a detailed understanding of the fate of transplanted cells. MRI is the most promising non-invasive and high resolution method for tracking live stem cells *in vivo* using cells prelabeled with SPIO (Siow et al., 2012). SPIO is a novel magnetic resonance contrast agent that produces negative contrast effects on T2-weighted sequences. In the present study, typical regions of hypointense signal were observed in the HPF-labeled hADSCs group at 1 day post-injection, which persisted for at least 4 weeks in T2WI images. We also found a stronger reaction (lower signal change and darker appearance) in enhanced susceptibility-weighted angiography images. Enhanced susceptibility-weighted angiography is a new MRI technique that exploits the magnetic susceptibility differences of iron in various tissues (Gang et al., 2013). Zhang et al. (2010) reported that iron concentrations in the substantia nigra of Parkinson's disease patients were the most significantly associated with symptomatic progression. Three-dimensional-enhanced susceptibility-weighted angiography was also recently suggested as a potential diagnostic technique for Parkinson's disease patients (Wang et al., 2013). We found that enhanced susceptibility-weighted angiography imaging provided better sensitivity and contrast for tracking HPF-labeled hADSCs compared with T2WI in routine MRI.

Our method also allowed detection of SPIO-labeled cells in much lower numbers (1×10^4 cells) than that previously reported in a rat stroke model (5×10^5 cells) (Shichinohe et al., 2013). Unlabeled-hADSCs transplanted rats also demonstrated a smaller hypointense signal only at 1 day after engraftment. The most likely explanation for the smaller reduction in signal intensity is the presence of iron-containing hemosiderin and deoxyhemoglobin decomposed from small hematoma induced by the injection procedure (Hu et al., 2012). In a study by Modo et al. (2012), neural stem cells were reported to migrate towards a stroke lesion regardless of whether they were transplanted in the ipsilateral or contralateral hemispheres. However, a greater number of neural stem cells were recruited around the lesion site when ipsilateral injection was used rather than contralateral injection. In the present study, hADSCs transplanted in the lesion boundary were not expected to migrate far from the site of injection. Indeed, histological examination with Prussian blue staining showed that the majority of cells remain at or near the injection site, even after 28 days after injection, with a small numbers of cells migrating into the cortex and along the subarachnoid space. This migration towards areas of injury may relate to the release of chemo-attractants by the lesion that attract transplanted stem cells (Barkho and Zhao, 2011).

In summary, we describe a simple protocol for efficient labeling of hADSCs with ferumoxytol, and demonstrate the feasibility of tracking low numbers of transplanted HPF-labeled hADSCs by 3.0 T MRI *in vivo*. The present study strongly suggests the therapeutic potential of transplanted hADSCs for ischemic stroke. These results may facilitate future development and non-invasive monitoring of stem cell-based therapies for clinical approaches.

Author contributions: *YY was responsible for experimental design and evaluation, data processing, integration and analysis, and paper writing. XZ was responsible for animal surgery. XG participated in cell preparation. YL provided technical support. CBJ and JL guided the study and provided technical and material support. All authors approved the final version of the paper.*
Conflicts of interest: *None declared.*

References

Arbab AS, Janic B, Haller J, Pawelczyk E, Liu W, Frank JA (2009) In vivo cellular imaging for translational medical research. Curr Med Imaging Rev 5:19-38.

Arslan F, Lai RC, Smeets MB, Akeroyd L, Choo A, Aguor EN, Timmers L, van Rijen HV, Doevendans PA, Pasterkamp G, Lim SK, de Kleijn DP (2013) Mesenchymal stem cell-derived exosomes increase ATP levels, decrease oxidative stress and activate PI3K/Akt pathway to enhance myocardial viability and prevent adverse remodeling after myocardial ischemia/reperfusion injury. Stem Cell Res 10:301-312.

Barkho BZ, Zhao X (2011) Adult neural stem cells: response to stroke injury and potential for therapeutic applications. Curr Stem Cell Res Ther 6:327-338.

Castaneda RT, Khurana A, Khan R, Daldrup-Link HE (2011) Labeling stem cells with ferumoxytol, an FDA-approved iron oxide nanoparticle. J Vis Exp 4:e3482.

Chen J, Sanberg PR, Li Y, Wang L, Lu M, Willing AE, Sanchez-Ramos J, Chopp M (2001) Intravenous administration of human umbilical cord blood reduces behavioral deficits after stroke in rats. Stroke 32:2682-2688.

Cho YJ, Song HS, Bhang S, Lee S, Kang BG, Lee JC, An J, Cha CI, Nam DH, Kim BS, Joo KM (2012) Therapeutic effects of human adipose stem cell-conditioned medium on stroke. J Neurosci Res 90:1794-1802.

Cromer Berman SM, Kshitiz, Wang CJ, Orukari I, Levchenko A, Bulte JW, Walczak P (2013) Cell motility of neural stem cells is reduced after SPIO-labeling, which is mitigated after exocytosis. Magn Reson Med 69:255-262.

De Feo D, Merlini A, Laterza C, Martino G (2012) Neural stem cell transplantation in central nervous system disorders: from cell replacement to neuroprotection. Curr Opin Neurol 25:322-333.

Del Zoppo GJ, Saver JL, Jauch EC, Adams HP Jr, American Heart Association Stroke Council (2009) Expansion of the time window for treatment of acute ischemic stroke with intravenous tissue plasminogen activator: a science advisory from the American Heart Association/American Stroke Association. Stroke 40:2945-2948.

Delcroix GJ, Jacquart M, Lemaire L, Sindji L, Franconi F, Le Jeune JJ, Montero-Menei CN (2009) Mesenchymal and neural stem cells labeled with HEDP-coated SPIO nanoparticles: in vitro characterization and migration potential in rat brain. Brain Res 1255:18-31.

Edmundson M, Thanh NT, Song B (2013) Nanoparticles based stem cell tracking in regenerative medicine. Theranostics 3:573-582.

Egashira Y, Sugitani S, Suzuki Y, Mishiro K, Tsuruma K, Shimazawa M, Yoshimura S, Iwama T, Hara H (2012) The conditioned medium of murine and human adipose-derived stem cells exerts neuroprotective effects against experimental stroke model. Brain Res 1461:87-95.

Emborg ME, Liu Y, Xi J, Zhang X, Yin Y, Lu J, Joers V, Swanson C, Holden JE, Zhang SC (2013) Induced pluripotent stem cell-derived neural cells survive and mature in the nonhuman primate brain. Cell Rep 3:646-650.

Fiedler T, Salamon A, Adam S, Herzmann N, Taubenheim J, Peters K (2013) Impact of bacteria and bacterial components on osteogenic and adipogenic differentiation of adipose-derived mesenchymal stem cells. Exp Cell Res 319:2883-2892.

Franco EC, Cardoso MM, Gouvêia A, Pereira A, Gomes-Leal W (2012) Modulation of microglial activation enhances neuroprotection and functional recovery derived from bone marrow mononuclear cell transplantation after cortical ischemia. Neurosci Res 73:122-132.

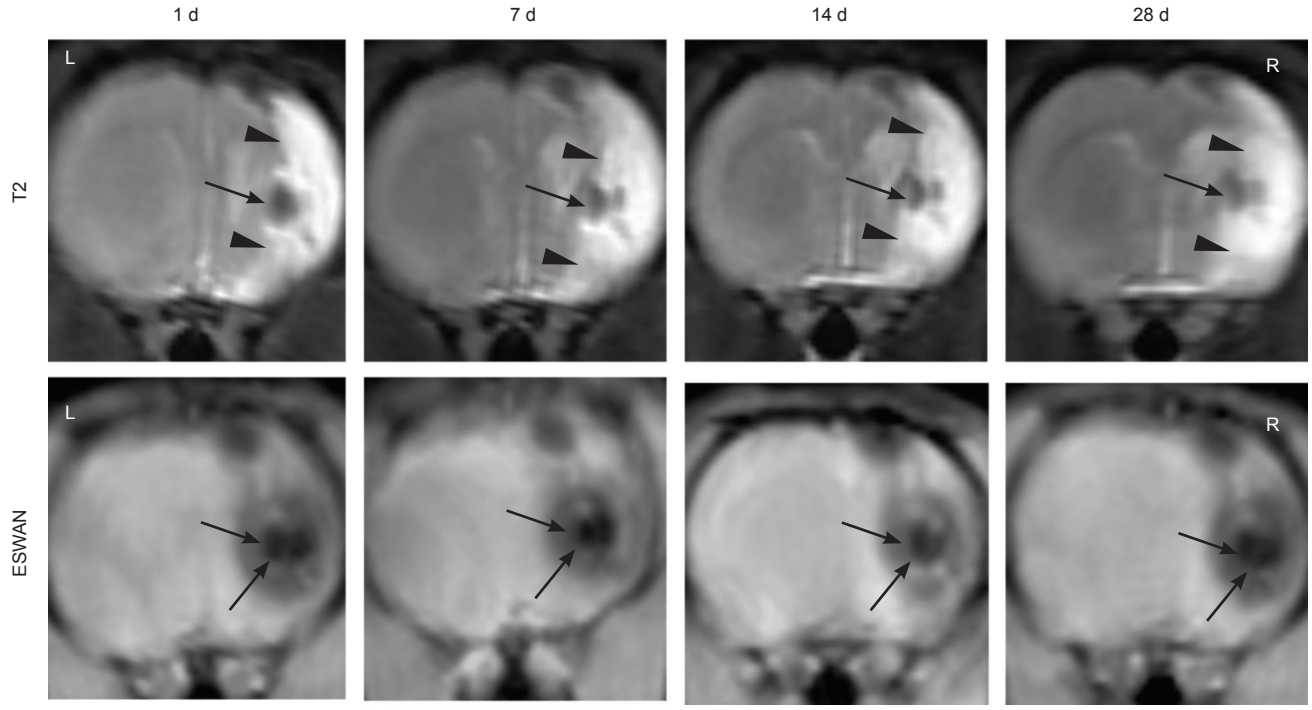

Figure 3 Serial magnetic resonance images of a representative rat treated with HPF-labeled hADSCs.
These images show the distribution of intracerebrally grafted hADSCs in the ischemic rat brain at 1, 7, 14, and 28 days after engraftment. Upper: T2-weighted images. Lower: ESWAN images. Arrowheads indicate the MCAO-induced lesion in the right hemisphere. Arrows indicate the signal loss area after stereotactic transplantation of the HPF-labeled hADSCs into the ipsilateral striatum. hADSCs: Human adipose-derived stem cells; HPF: ferumoxytol-heparin-protamine; ESWAN: enhanced susceptibility-weighted angiography; d: day(s); L: left; R: right.

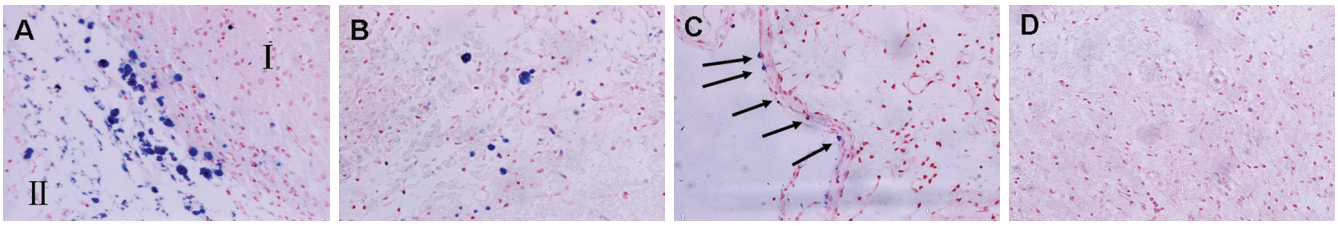

Figure 4 Distribution of Prussian blue-positive hADSCs at 28 days after ipsilateral striatum transplantation (Prussian blue staining, × 400).
Prussian blue-positive cells (arrows) were present in the injection site (the boundary of ischemia) (A: I, striatum; II, infarct tissue), infarct tissue (B), and the ipsilateral subarachnoid space (C) in the HPF-hADSCs group. No Prussian blue-positive cells were present in the PBS-treated group (D). hADSCs: Human adipose-derived stem cells; HPF: ferumoxytol-heparin-protamine.

Fu Y, Azene N, Xu Y, Kraitchman DL (2011) Tracking stem cells for cardiovascular applications in vivo: focus on imaging techniques. Imaging Med 3:473-486.
Gang Q, Zhang J, Hao P, Xu Y (2013) Detection of hypoxic-ischemic brain injury with 3D-enhanced T2 weighted angiography (ESWAN) imaging. Eur J Radiol 82:1973-1980.
Haddad-Mashadrizeh A, Bahrami AR, Matin MM, Edalatmanesh MA, Zomorodipour A, Fallah A, Gardaneh M, Ahmadian Kia N, Sanjarmoosavi N (2013) Evidence for crossing the blood barrier of adult rat brain by human adipose-derived mesenchymal stromal cells during a 6-month period of post-transplantation. Cytotherapy 15:951-60.
Hu SL, Lu PG, Zhang LJ, Li F, Chen Z, Wu N, Meng H, Lin JK, Feng H (2012) In vivo magnetic resonance imaging tracking of SPIO-labeled human umbilical cord mesenchymal stem cells. J Cell Biochem 113:1005-1012.
Huang B, Tabata Y, Gao JQ (2012) Mesenchymal stem cells as therapeutic agents and potential targeted gene delivery vehicle for brain diseases. J Control Release 162:464-473.
Huang W, Mo X, Qin C, Zheng J, Liang Z, Zhang C (2013) Transplantation of differentiated bone marrow stromal cells promotes motor functional recovery in rats with stroke. Neurol Res 35:320-328.
Inoue T, Sugiyama M, Hattori H, Wakita H, Wakabayashi T, Ueda M (2013) Stem cells from human exfoliated deciduous tooth-derived conditioned medium enhance recovery of focal cerebral ischemia in rats. Tissue Eng Part A 19:24-29.
Jensen MB, Yan H, Krishnaney-Davison R, Al Sawaf A, Zhang SC (2013) Survival and differentiation of transplanted neural stem cells derived from human induced pluripotent stem cells in a rat stroke model. J Stroke Cerebrovasc Dis 22:304-308.
Jin K, Xie L, Mao X, Greenberg MB, Moore A, Peng B, Greenberg RB, Greenberg DA (2011) Effect of human neural precursor cell transplantation on endogenous neurogenesis after focal cerebral ischemia in the rat. Brain Res 1374:56-62.
Kang SK, Lee DH, Bae YC, Kim HK, Baik SY, Jung JS (2003) Improvement of neurological deficits by intracerebral transplantation of human adipose tissue-derived stromal cells after cerebral ischemia in rats. Exp Neurol 183:355-366.
Kawabori M, Kuroda S, Sugiyama T, Ito M, Shichinohe H, Houkin K, Kuge Y, Tamaki N (2012) Intracerebral, but not intravenous, transplantation of bone marrow stromal cells enhances functional recovery in rat cerebral infarct: an optical imaging study. Neuropathology 32:217-226.

Kawabori M, Kuroda S, Ito M, Shichinohe H, Houkin K, Kuge Y, Tamaki N (2013) Timing and cell dose determine therapeutic effects of bone marrow stromal cell transplantation in rat model of cerebral infarct. Neuropathology 33:140-148.
Kim S, Chang KA, Kim Ja, Park HG, Ra JC, Kim HS, Suh YH (2012) The preventive and therapeutic effects of intravenous human adipose-derived stem cells in Alzheimer's disease mice. PLoS One 7:e45757.
Kocsis JD, Honmou O (2012) Bone marrow stem cells in experimental stroke. Prog Brain Res 201:79-98.
Kokaia Z, Martino G, Schwartz M, Lindvall O (2012) Cross-talk between neural stem cells and immune cells: the key to better brain repair? Nat Neurosci 15:1078-1087.
Leong WK, Henshall TL, Arthur A, Kremer KL, Lewis MD, Helps SC, Field J, Hamilton-Bruce MA, Warming S, Manavis J, Vink R, Gronthos S, Koblar SA (2012) Human adult dental pulp stem cells enhance poststroke functional recovery through non-neural replacement mechanisms. Stem Cells Transl Med 1:177-187.
Li L, Jiang Q, Ding G, Zhang L, Zhang ZG, Li Q, Panda S, Lu M, Ewing JR, Chopp M (2010) Effects of administration route on migration and distribution of neural progenitor cells transplanted into rats with focal cerebral ischemia, an MRI study. J Cereb Blood Flow Metab 30:653-662.
Liu Q, Wang LP, Yu J, Chen F, Diao B, Zhang Y (2014) Amplification of rabbit adipose-derived stem cells using explants culture method. Zhongguo Zuzhi Gongcheng Yanjiu 18:88-93.
Liu X (2012) Beyond the time window of intravenous thrombolysis: standing by or by stenting. Int Neurol 1:3-15.
Locatelli F, Bersano A, Ballabio E, Lanfranconi S, Papadimitriou D, Strazzer S, Bresolin N, Comi GP, Corti S (2009) Stem cell therapy in stroke. Cell Mol Life Sci 66:7577-7572.
Locke M, Windsor J, Dunbar PR (2009) Human adipose-derived stem cells: isolation, characterization and applications in surgery. ANZ J Surg 79:235-244.
Longa EZ, Weinstein PR, Carlson S (1989) Reversible middle cerebral artery occlusion without craniectomy in rats. Stroke 20:84-81.
Ma XW (2013) Embryonic stem cell transplantation for treatment of cerebrovascular diseases.Zhongguo Zuzhi Gongcheng Yanjiu 17:5717-5722.
Marconi S, Castiglione G, Turano E, Bissolotti G, Angiari S, Farinazzo A, Constantin G, Bedogni G, Bedogni A, Bonetti B (2012) Human adipose-derived mesenchymal stem cells systemically injected promote peripheral nerve regeneration in the mouse model of sciatic crush. Tissue Eng Part A 18:1264-1272.
McGuckin CP, Jurga M, Miller AM, Sarnowska A, Wiedner M, Boyle NT, Lynch MA, Jablonska A, Drela K, Lukomska B, Domanska-Janik K, Kenner L, Moriggl R, Degoul O, Perruisseau-Carrier C, Forraz N (2013) Ischemic brain injury: a consortium analysis of key factors involved in mesenchymal stem cell-mediated inflammatory reduction. Arch Biochem Biophys 534:88-97.
Mine Y, Tatarishvili J, Oki K, Monni E, Kokaia Z, Lindvall O (2013) Grafted human neural stem cells enhance several steps of endogenous neurogenesis and improve behavioral recovery after middle cerebral artery occlusion in rats. Neurobiol Dis 52:191-203.
Miyamoto M, Kuroda S, Zhao S, Magota K, Shichinohe H, Houkin K, Kuge Y, Tamaki N (2013) Bone marrow stromal cell transplantation enhances recovery of local glucose metabolism after cerebral infarction in rats: a serial 18F-FDG PET study. J Nucl Med 54:145-150.
Modo M, Stroemer RP, Tang E, Patel S, Hodges H (2002) Effects of implantation site of stem cell grafts on behavioral recovery from stroke damage. Stroke 33:2270-2278.
Nagai N, Kawao N, Okada K, Okumoto K, Teramura T, Ueshima S, Umemura K, Matsuo O (2010) Systemic transplantation of embryonic stem cells accelerates brain lesion decrease and angiogenesis. Neuroreport 21:575-579.
Oki K, Tatarishvili J, Wood J, Koch P, Wattananit S, Mine Y, Monni E, Tornero D, Ahlenius H, Ladewig J, Brüstle O, Lindvall O, Kokaia Z (2012) Human-induced pluripotent stem cells form functional neurons and improve recovery after grafting in stroke-damaged brain. Stem Cells 30:1120-1133.
Qi Y, Feng G, Huang Z, Yan W (2013) The application of super paramagnetic iron oxide-labeled mesenchymal stem cells in cell-based therapy. Mol Biol Rep 40:2733-2740.
Qu Y, Sun ZW, Yang DB, Jiang CL (2013) Neural stem cell transplantation for treatment of focal cerebral ischemia injury in rats. Zhongguo Zuzhi Gongcheng Yanjiu 17:1876-1883.
Rice HE, Hsu EW, Sheng H, Evenson DA, Freemerman AJ, Safford KM, Provenzale JM, Warner DS, Johnson GA (2007) Superparamagnetic iron oxide labeling and transplantation of adipose-derived stem cells in middle cerebral artery occlusion-injured mice. AJR Am J Roentgenol 188:1101-1108.
Savitz SI, Chopp M, Deans R, Carmichael T, Phinney D, Wechsler L (2011) Stem cell therapy as an emerging paradigm for stroke (STEPS) II. Stroke 42:825-829.
Schiller B, Bhat P, Sharma A (2014) Safety and effectiveness of ferumoxytol in hemodialysis patients at 3 dialysis chains in the United States over a 12-month period. Clin Ther 36:70-83.
Seyed Jafari SS, Ali Aghaei A, Asadi-Shekaari M, Nematollahi-Mahani SN, Sheibani V (2011) Investigating the effects of adult neural stem cell transplantation by lumbar puncture in transient cerebral ischemia. Neurosci Lett 495:1-5.
Shichinohe H, Yamauchi T, Saito H, Houkin K, Kuroda S (2013) Bone marrow stromal cell transplantation enhances recovery of motor function after lacunar stroke in rats. Acta Neurobiol Exp (Wars) 73:354-363.
Siow TY, Chen CC, Lin CY, Chen JY, Chang C (2012) MR phase imaging: sensitive and contrast-enhancing visualization in cellular imaging. Magn Reson Imaging 30:247-253.
Smith HK, Gavins FN (2012) The potential of stem cell therapy for stroke: is PISCES the sign? FASEB J 26:2239-2252.
Song M, Kim Y, Kim Y, Ryu S, Song I, Kim SU, Yoon BW (2009) MRI tracking of intravenously transplanted human neural stem cells in rat focal ischemia model. Neurosci Res 64:235-239.
Struys T, Ketkar-Atre A, Gervois P, Leten C, Hilkens P, Martens W, Bronckaers A, Dresselaers T, Politis C, Lambrichts I, Himmelreich U (2013) Magnetic resonance imaging of human dental pulp stem cells in vitro and in vivo. Cell Transplant 22:1813-1829.
Tae-Hoon L, Yoon-Seok L (2012) Transplantation of mouse embryonic stem cell after middle cerebral artery occlusion. Acta Cir Bras 27:333-339.
Thu MS, Bryant LH, Coppola T, Jordan EK, Budde MD, Lewis BK, Chaudhry A, Ren J, Varma NR, Arbab AS, Frank JA (2012) Self-assembling nanocomplexes by combining ferumoxytol, heparin and protamine for cell tracking by magnetic resonance imaging. Nat Med 18:463-467.
van Velthoven CT, van de Looij Y, Kavelaars A, Zijlstra J, van Bel F, Huppi PS, Sizonenko S, Heijnen CJ (2012) Mesenchymal stem cells restore cortical rewiring after neonatal ischemia in mice. Ann Neurol 71:785-796.
Wang C, Fan G, Xu K, Wang S (2013) Quantitative assessment of iron deposition in the midbrain using 3D-enhanced T2 star weighted angiography (ESWAN): a preliminary cross-sectional study of 20 Parkinson's disease patients. Magn Reson Imaging 31:1068-1073.
Wei L, Fraser JL, Lu ZY, Hu X, Yu SP (2012) Transplantation of hypoxia preconditioned bone marrow mesenchymal stem cells enhances angiogenesis and neurogenesis after cerebral ischemia in rats. Neurobiol Dis 46:635-645.
Wei X, Du Z, Zhao L, Feng D, Wei G, He Y, Tan J, Lee WH, Hampel H, Dodel R, Johnstone BH, March KL, Farlow MR, Du Y (2009) IFATS collection: The conditioned media of adipose stromal cells protect against hypoxia-ischemia-induced brain damage in neonatal rats. Stem Cells 27:478-488.
Zhang EF, Cao R, Xu T, Wang XY, Maierdan Maimaiti, Wang GQ, Sheng WB (2014) Comparative study of proliferative and neurosphere differentiation capacities of adipose-derived mesenchymal stem cells at different passages. Zhongguo Zuzhi Gongcheng Yanjiu 18:3030-3035.
Zhang J, Zhang Y, Wang J, Cai P, Luo C, Qian Z, Dai Y, Feng H (2010) Characterizing iron deposition in Parkinson's disease using susceptibility-weighted imaging: an in vivo MR study. Brain Res 1330:124-130.
Zuk PA, Zhu M, Mizuno H, Huang J, Futrell JW, Katz AJ, Benhaim P, Lorenz HP, Hedrick MH (2001) Multilineage cells from human adipose tissue: implications for cell-based therapies. Tissue Eng 7:211-228.

Copyedited by Dean J, Wysong S, Wang J, Qiu Y, Li CH, Song LP, Zhao M